Molecular and Cellular Biochemistry (2023) 478:743–754
https://doi.org/10.1007/s11010-022-04521-1

CircEXOC5 facilitates cell pyroptosis via epigenetic suppression of Nrf2 in septic acute lung injury

Wei Wang[1,3] · Yuqing Xiong[1] · Haomiao Zhao[1] · Rongli Xu[2]

Received: 16 December 2021 / Accepted: 5 July 2022 / Published online: 8 September 2022

Abstract

Acute lung injury (ALI) caused by sepsis is characterized by a destructive high inflammatory response in lungs, which is the ultimate cause of high mortality to patients diagnosed with sepsis. The objective of the present study is to explore the effect and related mechanisms of circEXOC5 on pyroptosis in septic ALI. Sepsis ALI mouse model was induced and established by CLP induction and sepsis MPVEC cell model by LPS. HE staining was used to detect lung tissue pathological changes. ELISA, flow cytometry, and Western blot were utilized to evaluate the release of inflammatory cytokines and cell pyroptosis, and RIP was applied to verify the binding relationship between EZH2 and circEXOC5 or Nrf2. Finally, the interaction between CircEXOC5 and EZH2, H3k27me3, and Nrf2 promoter regions was clarified using ChIP. CircEXOC5 levels were notably ascended in the lung tissues of septic ALI mice. And silencing circEXOC5 inhibited cell pyroptosis and the release of inflammatory cytokines in MPVEC stimulated by LPS. In addition, RIP and ChIP indicated that Nrf2 expression in MPVECs cells could be inhibited by circEXOC5 via recruiting EZH2. In addition, ML385 (a specific inhibitor of Nrf2) reversed the efficacy of Knockdown of circEXOC5 on the Inhibition of pyroptosis and inflammation of MPVEC cells stimulated by LPS. These results indicated that CircEXOC5 could promote cell pyroptosis through epigenetic inhibition of Nrf2 in septic ALI.

Keywords Sepsis · ALI · CircEXOC5 · Nrf2 · Cell pyroptosis

Abbreviations

ALI	Acute lung injury
circRNA	Circular RNA
EXOC5	Exocyst complex component 5
NLRP3	Recombinant NLR Family, Pyrin Domain Containing Protein 3
CLP	Cecal ligation and puncture
qRT-PCR	Quantitative real-time polymerase chain reaction
DMEM	Dulbecco's modified eagle medium
RIP	RNA immunoprecipitation
ChIP	Chromatin immunoprecipitation

Introduction

Sepsis is a life-threatening disease and defined as "life-threatening caused by the host's unbalanced response to infection organ dysfunction" in accordance with the third international consensus definition of sepsis and septic shock (Sepsis-3) [1, 2]. Lungs are particularly vulnerable to injury when sepsis occurs, and over half of the patients diagnosed with sepsis will worsen into acute lung injury (ALI) [3]. In the course of sepsis-induced ALI progression, the activation of inflammation and apoptosis pathways can result in destruction of alveolar epithelial cells, causing increased epithelial permeability and influx of edema fluid into the alveolar space [4, 5], which suggested that strategies to regulate inflammation and apoptosis pathways may provide

Wei Wang and Yuqing Xiong are the co-first authors.

✉ Wei Wang
Ww7411@126.com

1 Department of General Practice, Hainan General Hospital, Hainan Affiliated Hospital of Hainan Medical University, No.19, Xiuhua Road, Haikou 570311, Hainan Province, People's Republic of China

2 Department of Cardiology, Hainan General Hospital, Hainan Affiliated Hospital of Hainan Medical University, Haikou 570311, Hainan Province, People's Republic of China

3 Key Laboratory of Emergency and Trauma, Ministry of Education, Key Laboratory of Hainan Trauma and Disaster Rescue, The First Affiliated Hospital of Hainan Medical University, College of Emergency and Trauma, Hainan Medical University, Haikou 571199, Hainan Province, People's Republic of China

new opportunities for improving ALI induced by sepsis. However, the specific pathophysiological mechanism of sepsis-induced ALI is not yet clear and the effective method to which is not available at present. Therefore, exploring the mechanism and effective therapeutic targets of ALI caused by sepsis is the focus of current research.

The role of inflammatory dysregulation in the pathogenesis of ALI has been widely recognized, and it is mainly related to the imbalance of the massive release of inflammatory factors from crude salt [6]. When sepsis occurs, NOD-like receptor thermal protein domain-associated protein 3 (NLRP3) can be activated, and inflammatory bodies represented by NLRP3 further cleave and activate caspase 1. Typical pyroptosis is a caspase 1-dependent death in cells with essential features of production of pro-inflammatory cytokines and rapid plasma membrane rupture [7]. Recent studies indicated that alveolar macrophages and the pyroptosis of pulmonary vascular endothelial cells were of great significance in ALI progression [8, 9]. Moreover, studies have found that Ac-YVAD-CMK, a specific caspase 1 inhibitor, could attenuate LPS-induced lung injury activation and pyroptosis of mice via inhibition of caspase 1 [10]. Accordingly, inhibition of pyroptosis is likely to prevent or cure sepsis in future clinical practice.

Nrf2 (nuclear factor erythropoietin-2-related factor 2), an alkaline leucine zipper redox-sensitive transcription factor with anti-inflammatory properties and antioxidant, is the main controller and activator of dozens of cytoprotective genes, such as blood oxygenase-1 (HO-1), effectively resisting oxidative stress and inflammation [11]. Meanwhile, studies have also found that activating Nrf2/HO-1 signaling pathway could inhibit NLRP3 inflammasome-dependent pyroptosis [12, 13]. Researchers have found that the protection of artesunate on septic lung injury was associated with HO-1 induction which was regarded as the main anti-inflammatory enzyme controlled by Nrf2 activation [14]. Therefore, Nrf2 may be relevant to the initiation and progression of septic lung injury.

Circular RNA (circRNA), an endogenous non-coding RNA newly discovered with a closed-loop structure, is essential in regulating normal physiology along with pathological developments. In the last couple of years, circRNA has gradually been noticed being vital to sepsis-induced ALI. For instance, study [15] once reported that CircC3P1 attenuated the production of pro-inflammatory cytokines in sepsis-induced ALI by regulating miR-21 and apoptosis. Circ_0004399 (CircEXOC5) is the latest molecule that is highly expressed in ALI induced by sepsis through gene sequencing analysis [16]. However, its role in sepsis-induced ALI and its molecular mechanisms are still unclear.

Based on studies mentioned above, we speculated that circEXOC5 was highly expressed in sepsis-induced ALI and that knockdown of circEXOC5 could inhibit pyroptosis, thereby alleviating sepsis-induced ALI. In the present study, we further analyzed its related mechanisms in sepsis-induced ALI to seek for related new potential therapeutic targets.

Methods

Construction of sepsis ALI animal model

Adult male C57BL/6 mice (Charles River Laboratories, Beijing, China) were kept under a regulated environment of 22–24 °C, with a 12-h light–dark cycle and 60% humidity and were provided with water and food ad libitum. After one week of acclimatization, mice selected were randomly divided into sham group and model group, 20 mice each. Sepsis-induced ALI mouse model was established in model group through cecal ligation and puncture (CLP) with following specific operations: After anaesthetization with 10% chloral hydrate (3 mL/kg) on abdomen, mice were fixed in the supine position on the operating table. Cecum was exposed using a 0.5-cm longitudinal midline incision, and it was ligated 1 cm from the tip and then puncture was conducted once with 20-gauge needle at 0.5 cm from the ligation site. After gentle squeeze of cecum for a small amount of feces, mice intestine was re-positioned in their abdominal cavity with abdominal muscle tissue, peritoneum, and skin closed. Subsequently, hypodermic injection of normal saline was instantly offered. Apart from cecal ligation or puncture, mice in Sham group underwent the same operation described above. Experiments conducted in the present study were admitted by the animal ethics committee of our hospital.

HE staining for detection of pathological changes in lung tissues

All mice were euthanized (cervical dislocation) 3 days after surgery, and lung tissues were collected immediately for histopathological examination. Paraffin-embedded tissues were cut into sections with 5 μm each, stained with hematoxylin and eosin (H&E), and observed with a light microscope (magnification ×400). The degree of lung injury was assessed by lung injury score [17]. Scores are given by a comprehensive assessment of pulmonary hemorrhage, alveolar wall thickening, alveolar structural changes, hyaline membrane formation, and inflammatory cell infiltration: 0 indicates normal; 1 indicates mild injury; 2 indicates moderate injury; 3 indicates severe injury; and 4 indicates very severe histological changes.

Cell culture and transfection

The primary mouse pulmonary microvascular endothelial cells (MPVECs, 1×10^6/mL) were cultured in DMEM (Gibco, USA) by previous method. To set up an overexpression of circEXOC5 vector, we cloned circEXOC5 sequence into a PKCDH circular vector (RiboBio, China). Negative control vector was provided by GenePharm (Shanghai, China). Then, both circEXOC5 and empty vector were transfected into cells with Lipofectamine 2000 (Invitrogen, USA). 24 h after transfection, MPVEC was put into contact with lipopolysaccharide (LPS, 1 mg/mL) purchased from Sigma-Aldrich. Lastly, expression of related factors in the cells was evaluated 6 h after LPS treatment.

Enzyme-linked immunosorbent assay (ELISA)

Cells (1×10^5/well) were seeded into 6-well plates and treated as corresponding protocol. Then, cell supernatants were collected for cytokine detection. For in vivo assay, lung tissues were homogenized and centrifuged (14,000×*g*, 5 min) to collect the supernatants. Corresponding ELISA kit (USCN Life Science, Wuhan, China) was applied to assess the levels of interleukin-18 (IL-18) and IL-1β in cell culture supernatants and tissue samples.

Flow cytometry for cell pyroptosis detection

Cells were seeded into 6-well plates at a density of 1×10^6 cells/well. After the cells were pretreated, the supernatant was aspirated and cells of each group were rinsed twice with 10 mmol/L PBS. Later, we treated the cells with cell digestion solution without EDTA. With the deformation of cells and disappearance of cells connection, the digestion was terminated with complete culture medium and cells were then gently pipetted to fall off from the six-well plate wall in a sandy shape. Then after transferring the cell suspension to a sterile centrifuge tube, we centrifuged it for 5 min at 800 rpm with supernatant discarded. Afterward, it was resuspended by adding 10 mmol/L PBS and washed twice. Subsequently, we aspirated and discarded the supernatant, resuspended the cells, and adjusted the number of cells to 1×10^6 cells/mL. 100 μL of cell suspension was taken and placed in a dedicated flow tube with 5 μL PI and 5 μL Annexin V-FITC added successively in the dark for mixture and then incubated for 15 min under room temperature away from light. 400 μL 1 × Binding Buffer should be added for resuspension of cells before using the machine and the test should be performed within 30 min. BD FAC-SDiva.8 software was used for data analysis. The percentage of AnnexinV-FITC$^+$/PI$^+$ double-positive cells was applied as the pyroptosis rate. Experiment stated above was conducted repeatedly for three times.

Fluorescence staining for ROS detection

Production of intracellular ROS was detected with DCFH-DA (Beyotime, China) in the current step. Seeded in a 6-well plate with DCFH-DA (10 μM) added, the cells (1.5×10^5 cells/well) were then incubated at 37 °C away from the light and washed 3 times with PBS. And ROS was detected by a fluorescence microscope (OLYMPUS IX73, Tokyo, Japan) and captured by OLYMPUS cellSens Standard 1.17 under room temperature in the dark. The experiment was repeated three times.

qRT-PCR detection

Cells were seeded in 24-well plates at a density of 1×10^5 cells per well, then cultured, and treated. Total RNA was extracted from MPVECs and mouse lung tissues with TRIzol (Invitrogen, CA, USA). The transcription of RNA was reversed to cDNA with PrimeScript™ RT Master Mix (Takara, China) following the manufacturer's instructions. circEXOC5 level was detected by Roche Light Cycler 480 Real-time PCR Amplifier according to kit instructions. The reaction conditions were as follows: 95 °C pre-denaturation for 2 min, 95 °C amplification for 15 s, and 60 °C annealing for 1 min, with a total of 40 cycles of above steps. GAPDH was served as an internal control and $2^{-\Delta\Delta Ct}$ was for data analysis. circEXOC5: Forward primer: 5′-AGAGTTCCT TGAGCTTGAAATGA-3′, Reverse primer: 5′-CCATGT GGCCTGGACAAAAC-3′ and GAPDH: Forward primer: 5′-CCTTCCGTGTCCCCA CT-3′, Reverse primer: 5′-GCC TGCTTCACCACCTTC-3′.

Western blot

Total protein isolated from mouse lung tissues and MPVECs (2×10^6 cells/well in 6-well plates for culture and treatment) was lysed by RIPA lysis buffer (Beyotime, China), and BCA protein assay kit (Beyotime, P0010, China) was utilized to detect the protein concentration. After separating 40–80 μg of protein on a 10% SDS-PAGE gel, we transferred it to a polyvinylidene fluoride (PVDF) membrane (MilliporeSigma, Burlington, USA) and sealed for subsequent operation. Later, PVDF membrane was incubated at 4 °C for 12 h along with NLRP3 (1:1000, ab214185), ASC (1:1000, ab283684), cleaved caspase 1 (1:2000, ab32503), Nrf2 (1:2000, ab32503), HO-1 (1:2000, ab32503), and β-actin (1:1000, ab8226) primary antibody (Abcam, Cambridge, UK) and then it was incubated along with the goat anti-rabbit secondary antibody (1:2000, ab6721) for 50 min. Alphalmager™ 2000 imaging system (Alpha Innotech, San Leandro, USA) was utilized for quantification of protein bands density.

RNA immunoprecipitation (RIP)

Magna RIP RBP immunoprecipitation kit (EMD Millipore) was applied for RIP determination. Cells (2×10^7) lysate was incubated with dynabeads coated with IgG antibody or AGO2 antibody for 12 h at 4 °C, and the complex of protein-RNA was captured and digested with proteinase K to extract RNA fraction. Later, we washed the magnetic beads repeatedly with RIP washing buffer to remove as much non-specific adsorption as possible and lastly subjected the extracted RNA to qRT-PCR.

Chromatin immunoprecipitation (ChIP)

ChIP was conducted strictly in accordance with the instruction of kit (Millipore). MPVECs (1×10^6) were used to evaluate the binding of EZH2 and H3K27me3 to the Nrf2 promoter. MPVECs were placed in the digestion buffer, then with 0.3 U of micrococcal nuclease (MNase; Sigma-Aldrich, St. Louis, MO) put into the solution, and then it was incubated under 37 °C for 5 min. After inactivating the reaction by incubating with 50 mM RIPA buffer and EDTA for 16 h, the solution was incubated with around 3 μg of H3K27me3 primary antibodies and EZH2 (#5246) along with dynabeads protein A beads (Invitrogen, #9733) at 4 °C for 16 h. For comparison, normal rabbit IgG (Santa Cruz sc-2025) was taken as a control. And its DNA was extracted and processed in accordance with the instructions of ChIP Kit used in PCR analysis. IgG was used as a control to determine the relative enrichment level in the current step.

Statistical analysis

SPSS19.0 was utilized to perform statistical analysis on data collected, and GraphPad 8 (GraphPad Software) was utilized to draw the required pictures. The *t* test was conducted for comparison between groups, one-way analysis of variance for that among multiple groups, and LSD *t* test was for post hoc comparison. $P < 0.05$ indicated notable difference.

Results

Sepsis lung injury facilitated cell pyroptosis and up-regulated the expression of circEXOC5

A mouse model of sepsis was constructed and the pathological lung tissue changes of the mice were detected by HE staining. It was found that the alveolar morphology of sham group mice was normal, while that in the CLP group showed vascular congestion, hemorrhage, collapse of alveolar sacs, and thickening of alveolar walls and alveolar

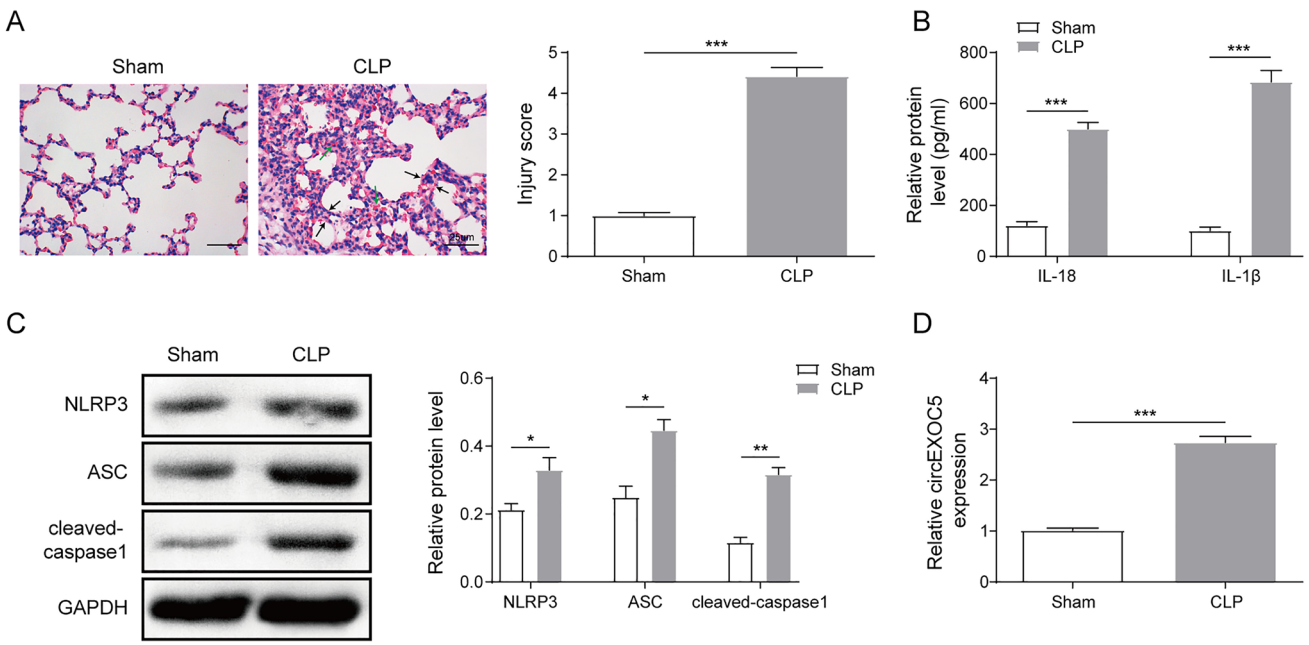

Fig. 1 Septic lung injury could promote pyroptosis and up-regulates the expression of circEXOC5. **A** Pathological changes in lung tissues of septic ALI mice were observed by HE staining, and the injury score of the mice was evaluated; **B** the expression of IL-18 and IL-1β in lung tissues of septic ALI mice were observed with ELISA; **C** protein expression of NLRP3, ASC, and cleaved Caspase 1 were detected with western blot; **D** expression of circEXOC5 in lung tissues of septic ALI mice was detected with qRT-PCR. $n = 6$, 6 tissues from 6 mice. $^*P < 0.05$, $^{**}P < 0.01$, $^{***}P < 0.001$. All the experiments were performed in triplicate

septa. In addition, the injury score of mice in CLP group was significantly higher than that in the Sham group (Fig. 1A). Compared to the sham group, levels of IL-18 and IL-1β in lung tissue of the CLP group mice showed significant increase via ELISA test (Fig. 1B), the protein expression of NLRP3, ASC, and cleaved caspase 1 in lung tissue of mice was detected with striking incline in CLP group via western blot (Fig. 1C), and qRT-PCR detection presented a drastic up-regulation of circEXOC5 in CLP group (Fig. 1D). Above results indicated that the sepsis ALI mouse model was established successfully, and expression of circEXOC5 could be up-regulated in sepsis ALI mice.

Silencing circEXOC5 inhibited LPS-induced pyroptosis of MPVECs cells

To analyze the effect of circEXOC5 on LPS-induced MPVECs cell pyroptosis, we transfected circEXOC5 shRNA and its negative control in MPVECs cells, and qRT-PCR results showed that compared to shNC group, transfection of shcircEXOC5 drastically declined the expression of circEXOC5 (Fig. 2A). After transfection, LPS was applied to induce MPVECs for stimulation of an in vitro injury model of sepsis, and fluorescent staining was for ROS level detection which revealed that LPS significantly promoted the cellular ROS level, while knocking down circEXOC5 strikingly reduced ROS generation when compared with control group (Fig. 2B). Subsequently, flow cytometry detected cell pyroptosis and indicated that pyroptosis was significantly increased after LPS induction, while knocking down circEXOC5 significantly inhibited pyroptosis (Fig. 2C). ELISA test results revealed that levels of IL-18 and IL-1β in cells of LPS group were notably increased, while significantly reduced with knockdown of circEXOC5 (Fig. 2D). Western blot results showed that the expression of NLRP3, ASC, and cleaved caspase 1 presented notable rise in LPS group, while knocking down circEXOC5 significantly reversed the expression of the above pyroptosis-related proteins (Fig. 2E). Results above indicated that silencing circEXOC5 could effectively inhibit LPS-induced pyroptosis of MPVEC cells.

circEXOC5 apparently inhibited the expression of Nrf2 by recruiting EZH2

Then, the mechanism by which circEXOC5 regulates downstream pathways and cell functions was investigated. Western blot was for detection of EZH2 and H3k27me3 expression, which indicated that in comparison with the control group, expression of EZH2 and H3k27me3 in the LPS group was increased strikingly, while knocking down circEXOC5 significantly down-regulated the expression of H3k27me3 and EZH2 (Fig. 3A). RIP detection of the binding between circEXOC5 and EZH2 indicated that, compared with the IgG treatment group, RIP enrichment of CircEXOC5 in the EZH2 antibody treatment group was drastically enhanced (Fig. 3B). ChIP was utilized to detect the expression of the Nrf2 promoter, showing that compared with the shNC group, the accumulation of EZH2 and H3K27me3 in Nrf2 promoter region was declined notably after circEXOC5 was knocked out (Fig. 3C). Subsequently, to prove whether circEXOC5 could apparently inhibit the expression of Nrf2 by recruiting EZH2, we over-expressed circEXOC5 and inhibited the expression of EZH2 in MPVECs simultaneously, showing that compared with vector, overexpression of circEXOC5 strikingly inhibited the expression of Nrf2, while knocking down EZH2 partially restored the expression of Nrf2 (Fig. 3D). Above results indicated that circEXOC5 could inhibit Nrf2 expression in MPVECs by recruiting EZH2.

circEXOC5 could promote LPS-induced MPVEC pyroptosis by regulating the Nrf2/HO-1 signaling pathway

To further investigate the effect of Nrf2/HO-1 pathway on circEXOC5 regulating MPVEC pyroptosis, we introduced ML385 (Nrf2-specific inhibitor). And fluorescence staining was used for detection of ROS level, which revealed that ROS level induced by LPS was reduced significantly by silencing circEXOC5 and reversed markedly by Nrf2 inhibitor treatment (Fig. 4A). Results of flow cytometry detection of cell pyroptosis showed that silencing circEXOC5 notably declined LPS-induced pyroptosis, while Nrf2 inhibitor treatment significantly rose cell pyroptosis (Fig. 4B). ELISA test results showed that silencing circEXOC5 strikingly inhibited the expression of IL-1β and IL-18 induced by LPS, while treatment with ML385 notably increased the content of IL-1β and IL-18 (Fig. 4C). Finally, western blot detection showed that LPS induced down-regulation of Nrf2 and HO-1 expression while promoted that of NLRP3, ASC, and cleaved caspase 1 when compared with the control group. However, knocking down circEXOC5 significantly accelerated the expression of HO-1 and Nrf2 and inhibited that of NLRP3, ASC, and cleaved caspase 1. Furthermore, when ML385 treatment was conducted after the knockdown, the expression of above proteins was significantly reversed (Fig. 4D). Above results suggested that circEXOC5 could promote LPS-induced MPVEC pyroptosis by regulating the Nrf2/HO-1 signaling pathway.

Silencing circEXOC5 could relieve septic lung injury in vivo

To further verify the effect of circEXOC5 on septic lung injury at the animal level, we injected adenovirus (Ad)-sh

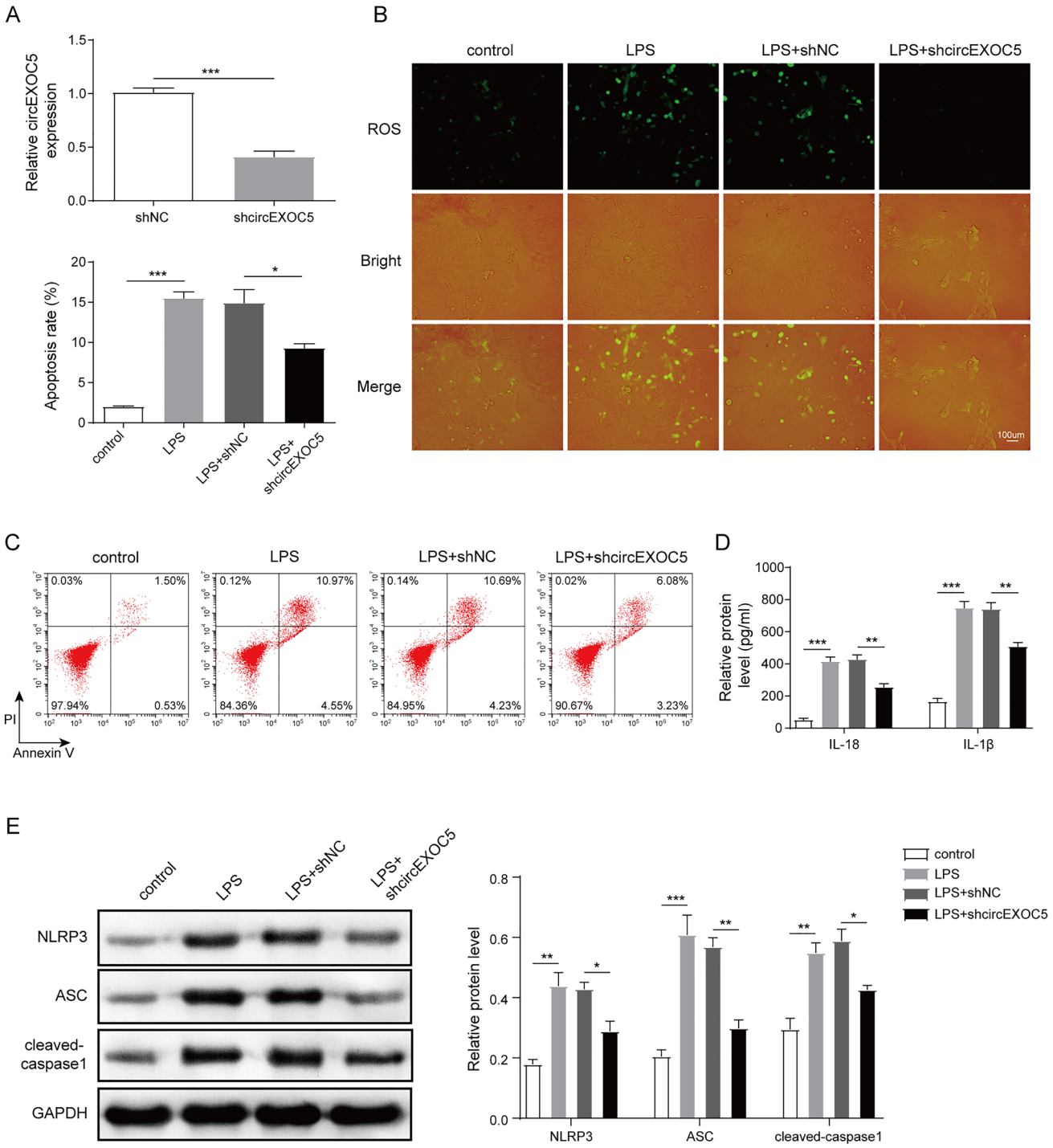

Fig. 2 Silencing circEXOC5 inhibited LPS-induced pyroptosis of MPVECs cells. **A** The transfection efficiency of shcircEXOC5 was detected with qRT-PCR; **B** the effect of shcircEXOC5 on ROS in MPVECs induced by LPS was detected with DCFH-DA fluorescence staining; **C** the pyroptosis of MPVECs induced by LPS after shcircEXOC5 transfection was detected with flow cytometry; **D** the expression of IL-18 and IL-1β in MPVECs cells induced by LPS after shcircEXOC5 transfection was detected with ELISA; (E) the expression of NLRP3, ASC, and cleaved caspase 1 protein in MPVECs induced by LPS after shcircEXOC5 transfection was detected with western blot. $n=3$. $^{*}P<0.05$, $^{**}P<0.01$, $^{***}P<0.001$. All the experiments were performed in triplicate

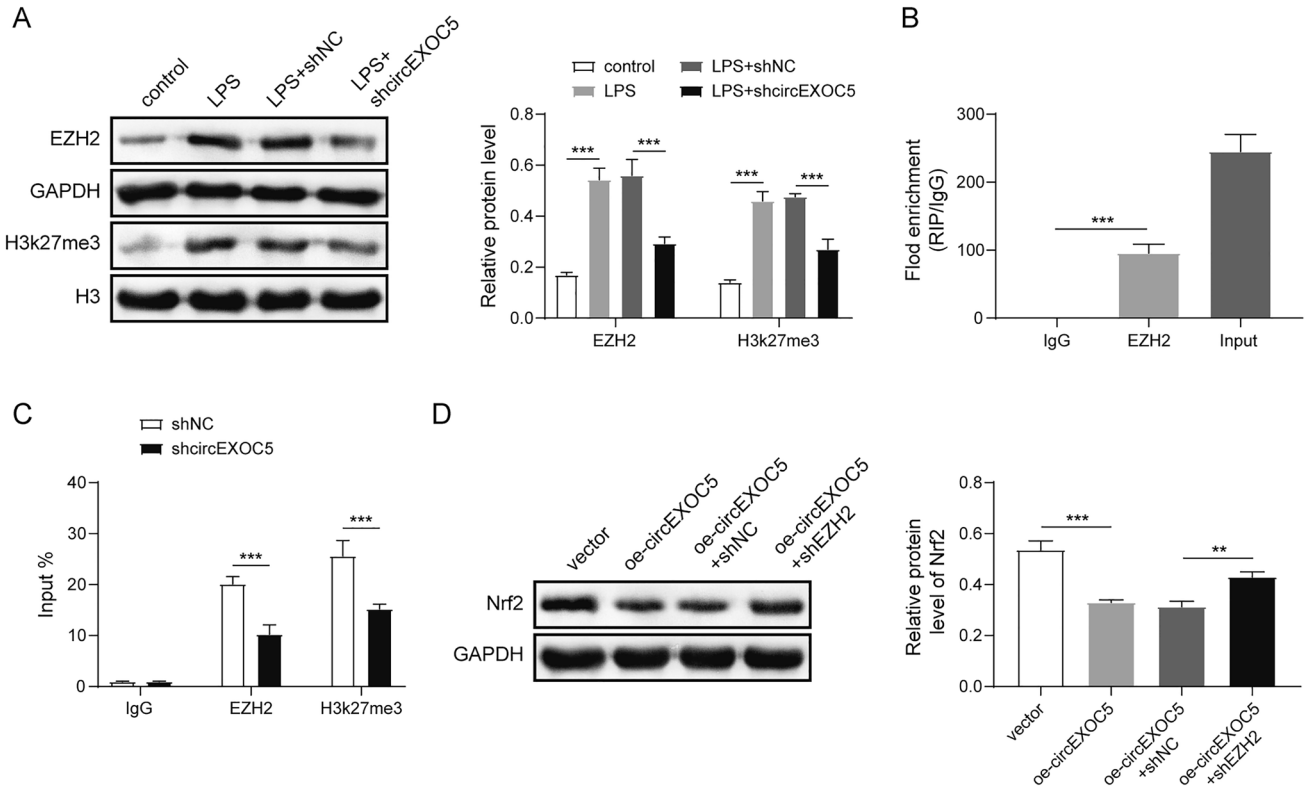

Fig. 3 circEXOC5 apparently inhibited the expression of Nrf2 by recruiting EZH2. **A** EZH2 and H3k27me3 expression in MPVECs induced by LPS after circEXOC5 shRNA transfection were detected with western blot; **B** the binding between circEXOC5 and EZH2 was detected with RIP; **C** expression of Nrf2 promoter was detected with ChIP; **D** The effect of circEXOC5 overexpression and simultaneous inhibition of EZH2 on Nrf2 expression in MPVECs cells. $n=3$. $^{**}P<0.01$, $^{***}P<0.001$. All the experiments were performed in triplicate

circEXOC5 or negative control (NC) into the tail vein according to the group one week before the establishment of the sepsis mouse model and conducted following comparison taking sham group as the control. Firstly, qRT-PCR was for detection of circEXOC5 expression, showing that the expression of circEXOC5 in CLP group was notably up-regulated, while knocking down circEXOC5 significantly reduced its own expression level (Fig. 5A). The measurement results of the lung dry weight ratio of the mice in each group suggested that the ratio in CLP group increased drastically, while knocking down circEXOC5 significantly reduced the lung dry weight ratio (Fig. 5B). HE staining was for detection of pathological changes in the lung tissue of mice, indicating that the alveolar morphology of sham group was normal, and mice in CLP group showed symptoms like vascular congestion, hemorrhage, alveolar sac collapse, and thickening of alveolar walls and alveolar septa and its Injury score was significantly higher than that of the sham group. After knocking down circEXOC5, the morphological changes of lung tissue in mice induced by CLP were significantly relieved, and the Injury score was significantly lower than that of the CLP + Ad-sh NC group. (Fig. 5C). ELISA test showed that the contents of IL-18 and IL-1β in the lung tissue of CLP mice increased strikingly, while knocking down circEXOC5 could significantly reduce them (Fig. 5D). Western blot results suggested that the expression of NLRP3, ASC, and cleaved caspase 1 was drastically promoted in the CLP group, while knocking down circEXOC5 significantly down-regulated the expression of the above pyroptosis-related proteins (Fig. 5E). Taken all together, silencing circEXOC5 could alleviate septic lung injury at the animal level.

Discussion

Sepsis, a systemic inflammatory response syndrome (SIRS) with complex causes, is most likely to result in multiple organ dysfunction syndrome (MODS) and mortality among critically ill patients [18]. ALI is characterized by a destructive and excessive inflammatory response in the lungs and is considered to be one of the most serious complications of sepsis, leading to a high mortality rate to sepsis patients [19]. In the present study, we established

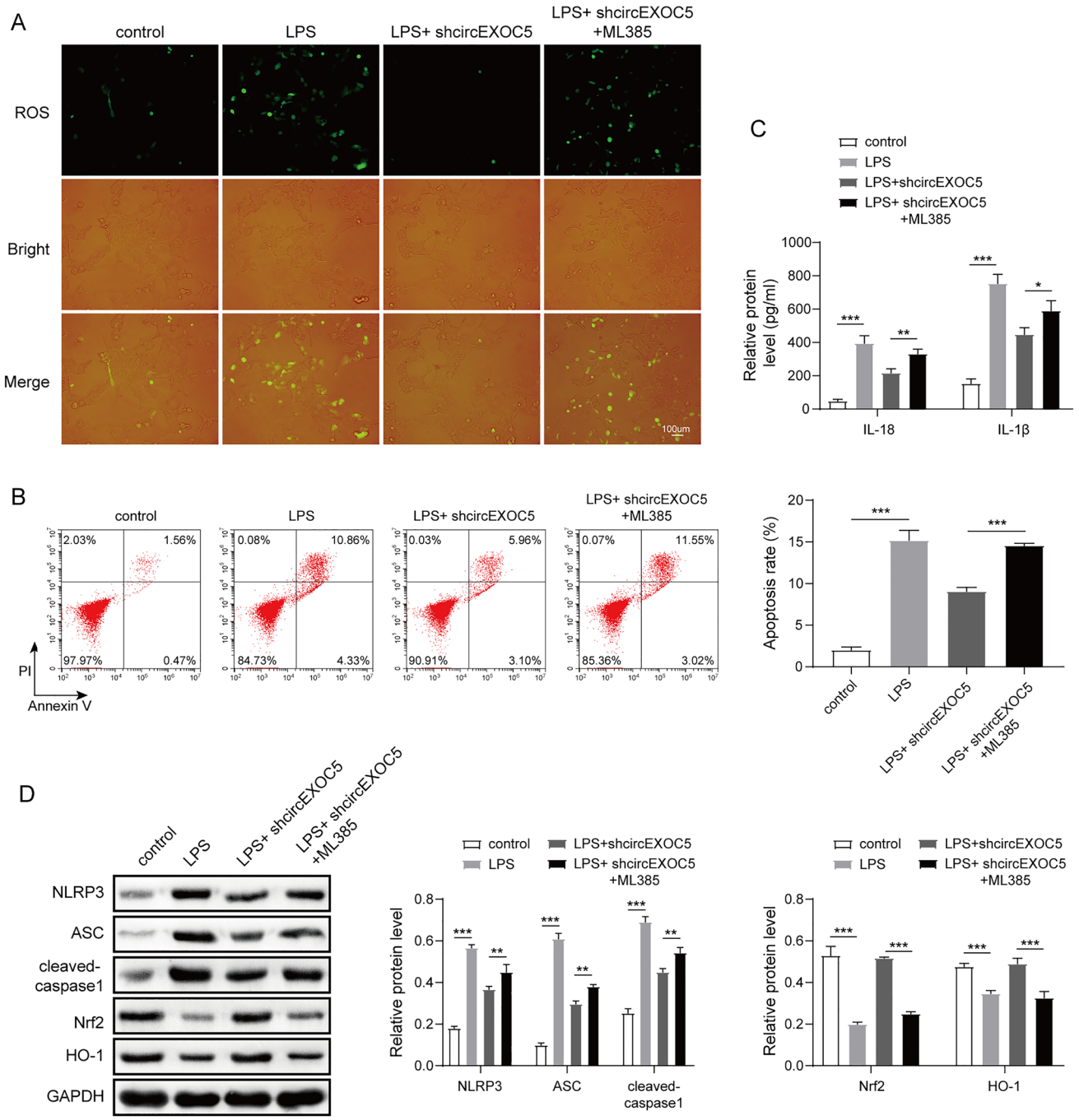

Fig. 4 circEXOC5 could promote MPVEC cell pyroptosis caused by LPS via regulating Nrf2/HO-1 signal. **A** ROS level in sepsis model cells transfected with circEXOC5 shRNA treated with ML385 was detected with DCFH-DA fluorescence staining; **B** the pyroptosis of sepsis model cells transfected with circEXOC5 shRNA treated by ML385 was detected with flow cytometry; **C** expression of IL-1β and IL-18 in sepsis model cells transfected with circEXOC5 shRNA treated with ML385 were detected using ELISA; **D** Nrf2, HO-1, NLRP3, ASC, and cleaved caspase 1 protein expression in sepsis model cells transfected with circEXOC5 shRNA treated by ML385 were detected with western blot. $n=3$. $^{*}P<0.05$, $^{**}P<0.01$, $^{***}P<0.001$. All the experiments were performed in triplicate

a sepsis-complicated ALI mouse model through CLP induction, and obvious ALI features were observed among the ALI mice, including hemorrhage, pulmonary edema, and excessive accumulation of inflammatory cell. It was also observed in ALI mice with activation of NLRP3 inflammasome, change of expression in pyroptosis-related proteins, and marked up-regulation of circEXOC5. Researches indicated that the increases of pyroptosis and

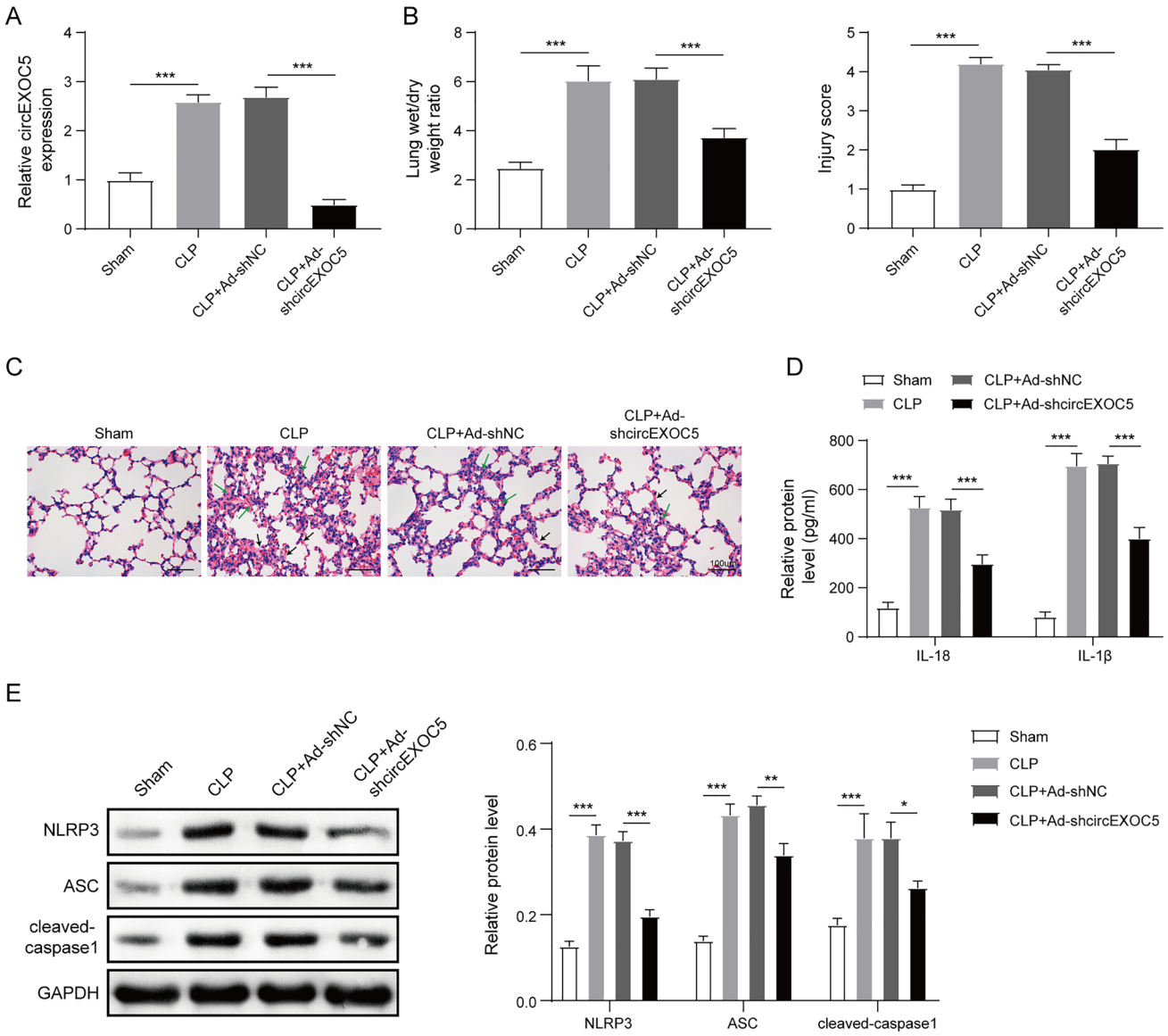

Fig. 5 Silencing circEXOC5 could alleviate septic lung injury at the animal level. **A** circEXOC5 expression in septic lung injury mice after Ad-shcircEXOC5 injection was detected with qRT-PCR; **B** The dry weight ratio measurement results of the lungs of each group of mice after Ad-shcircEXOC5 injection; **C** pathological changes of lung tissues in mice after Ad-shcircEXOC5 injection were detected with HE staining, and the injury score of the mice was evaluated; **D** changes in the levels of IL-1β and IL-18 in mouse lung tissues after Ad-shcircEXOC5 injection were detected using ELISA; (E) expression of NLRP3, ASC, and cleaved caspase 1 protein in lung tissues of mice after Ad-shcircEXOC5 injection were detected with western blot. $n=6$, 6 lung tissues from 6 mice. $^{*}P<0.05$, $^{**}P<0.01$, $^{***}P<0.001$. All the experiments were performed in triplicate

pro-inflammatory mediators played a vital role in the process of sepsis-induced ALI, and inhibition of inflammation and pyroptosis could improve sepsis-induced lung injury [20, 21]. And we also observed in the present study that circEXOC5 could promote pyroptosis through epigenetic inhibition of Nrf2 in septic ALI. This allowed us to see the potential therapeutic role of circEXOC5 in managing sepsis-induced ALI.

At present, the regulatory role and potential mechanisms of circRNA working in the pathogenesis of inflammation-related diseases have been widely discussed. For example, study once found that circRNA 103765 acted as a pro-inflammatory factor in Crohn's disease through sponge miR-30 [22]. There were also studies on sepsis showing that circRNA 0001105 could protect the intestinal barrier of septic rats by inhibiting YAP1 expression, oxidative damage, and inflammation [23]. At present, mouse lung microvascular endothelial cells stimulated by LPS have been widely used as an ALI cell model [24]. We also found that LPS could trigger the release of MPVECs cell pyroptosis and inflammatory cytokine levels, while silencing

circEXOC5 could significantly alleviate the pyroptosis and inflammation of MPVECs induced by LPS. Moreover, it was observed in animal experiments that silencing circEXOC5 significantly improved CLP-induced ALI in mice. In summary, above data indicated that silencing circEXOC5 could improve sepsis-induced ALI both in vivo and in vitro. Previous studies suggested that circRNAs were related to ALI [25]. For example, it was found that silencing circ_0054633 could alleviate LPS-induced ALI through NF-κB signaling pathway, which is consistent with our observation of how circRNAs works in ALI. And since the role of CircEXOC5 in sepsis has not been reported yet, we are the first to report the role of CircEXOC5 on sepsis-induced ALI.

It was previously reported that circRNA could regulate Nrf2 to regulate inflammation-related diseases. For example, Liu and his team found that Hsa_circ_0005915 could promote N, N-dimethylformamide-induced oxidative stress in HL-7702 cells via Nrf2/ARE axis [26]. In the present study, we verified the role of circEXOC5 working in septic ALI, which was observed to inhibit Nrf2 expression by recruiting EZH2 to Nrf2 promoter, thereby promoting the occurrence and development of septic ALI. Although silencing circEXOC5 did not change the overall expression level of EZH2, it was observed that the binding between Nrf2 promoter and EZH2 was reduced, which is of value in clinical practice and in urgent need of further research.

EZH2, the catalytic subunit of Polycomb Inhibitory Complex 2 (PRC2), can catalyze the production of trimethylated H3K27 (H3K27me3) from Lysine 27 (H3K27) of histone H3 [27]. Previous studies reported that EZH2 was observed to participate in the regulation of inflammation. For instance, it was suggested that EZH2 played a vital role in regulating microglia's essential genes for activating inflammation [28]. In addition, other studies have also shown that recruiting H3K27me3 to the promoter site of Nrf2 could inhibit Nrf2 transcription [29], which is similar to the mechanism we have observed. HO-1 can be activated by Nrf2 and have anti-apoptotic effects, antioxidant, and anti-inflammatory along with its metabolites [30]. Former studies have verified that HO-1 could play a protective role in lung injury induced by sepsis via protecting lungs from inflammation and oxidant-induced tissue damage [31, 32]. In addition, studies have found that overexpression of HO-1 could attenuate ROS production, thereby reducing neutrophil infiltration [33]. In our study, however, it was found that knocking down circEXOC5 notably promoted the expression of Nrf2 and HO-1, while ML385 treatment significantly inhibited the expression of Nrf2 and HO-1 protein, which suggested that HO-1 expression could be regulated by Nrf2, altogether proving that circEXOC5 could promote LPS-induced MPVECs cell pyroptosis by regulating the Nrf2/HO-1 signaling pathway. To our knowledge, this is the first report to reveal and emphasize the importance of EZH2 in regulating Nrf2 expression in septic ALI.

Conclusions

In summary, our current findings indicated that circEXOC5 was up-regulated in septic ALI. circEXOC5 could contribute to the activation of inflammasomes in septic ALI and regulate the Nrf2-mediated antioxidant response by interacting with EZH2, thereby promoting the occurrence of ALI. These findings indicated that circEXOC5 may be a potential target for clinical application of anti-septic ALI.

Acknowledgements We would like to give our sincere gratitude to the reviewers for their constructive comments.

Author contributions WW contributed to conceptualization, methodology, visualization, validation, supervision, writing and preparation of the original draft, investigation, and writing, reviewing, and editing of the manuscript. YX contributed to conceptualization, methodology, validation, writing and preparation of original draft preparation, and investigation. HZ assisted in data curation and software. RX performed visualization.

Funding This work was supported by National Natural Science Foundation of China No.82160359 (No. 82160359), Hainan Provincial Natural Science Foundation of China (No.822RC812), Hainan Provincial Medical and Health Research Project (No.21A200165) and Hainan Medical University Scientific Research Cultivation Foundation (No. HYPY201908).

Data availability Not applicable.

Declarations

Conflict of interest The authors declare that they have no conflict of interest.

Ethical approval All experiments conducted in the present study were approved by the animal ethics committee of our hospital.

Consent for publication Not applicable.

References

1. Singer M, Deutschman CS, Seymour CW, Shankar-Hari M, Annane D, Bauer M, Bellomo R, Bernard GR, Chiche JD, Coopersmith CM, Hotchkiss RS, Levy MM, Marshall JC, Martin GS, Opal SM, Rubenfeld GD, van der Poll T, Vincent JL, Angus DC (2016) The Third International Consensus definitions for sepsis and septic shock (sepsis-3). JAMA 315:801–810. https://doi.org/10.1001/jama.2016.0287
2. Levitt JE, Matthay MA (2010) The utility of clinical predictors of acute lung injury: towards prevention and earlier recognition. Expert Rev Respir Med 4:785–797. https://doi.org/10.1586/ers.10.78

3. Sevransky JE, Martin GS, Shanholtz C, Mendez-Tellez PA, Pronovost P, Brower R, Needham DM (2009) Mortality in sepsis versus non-sepsis induced acute lung injury. Crit Care 13:R150. https://doi.org/10.1186/cc8048
4. Johnson ER, Matthay MA (2010) Acute lung injury: epidemiology, pathogenesis, and treatment. J Aerosol Med Pulm Drug Deliv 23:243–252. https://doi.org/10.1089/jamp.2009.0775
5. Martin TR, Nakamura M, Matute-Bello G (2003) The role of apoptosis in acute lung injury. Crit Care Med 31:S184–S188. https://doi.org/10.1097/01.CCM.0000057841.33876.B1
6. Parsons PE, Eisner MD, Thompson BT, Matthay MA, Ancukiewicz M, Bernard GR, Wheeler AP, Network NARDSCT (2005) Lower tidal volume ventilation and plasma cytokine markers of inflammation in patients with acute lung injury. Crit Care Med 33:1–6. https://doi.org/10.1097/01.ccm.0000149854.61192.dc
7. Wang YC, Liu QX, Zheng Q, Liu T, Xu XE, Liu XH, Gao W, Bai XJ, Li ZF (2019) Dihydromyricetin alleviates sepsis-induced acute lung injury through inhibiting NLRP3 inflammasome-dependent pyroptosis in mice model. Inflamm 42:1301–1310. https://doi.org/10.1007/s10753-019-00990-7
8. Yang J, Zhao Y, Zhang P, Li Y, Yang Y, Yang Y, Zhu J, Song X, Jiang G, Fan J (2016) Hemorrhagic shock primes for lung vascular endothelial cell pyroptosis: role in pulmonary inflammation following LPS. Cell Death Dis 7:e2363. https://doi.org/10.1038/cddis.2016.274
9. Wu D, Pan P, Su X, Zhang L, Qin Q, Tan H, Huang L, Li Y (2016) Interferon regulatory factor-1 mediates alveolar macrophage pyroptosis during LPS-induced acute lung injury in mice. Shock 46:329–338. https://doi.org/10.1097/SHK.0000000000000595
10. Wu DD, Pan PH, Liu B, Su XL, Zhang LM, Tan HY, Cao Z, Zhou ZR, Li HT, Li HS, Huang L, Li YY (2015) Inhibition of alveolar macrophage pyroptosis reduces lipopolysaccharide-induced acute lung injury in mice. Chin Med J (Engl) 128:2638–2645. https://doi.org/10.4103/0366-6999.166039
11. Huang C, Zhang C, Yang P, Chao R, Yue Z, Li C, Guo J, Li M (2020) Eldecalcitol inhibits LPS-induced NLRP3 inflammasome-dependent pyroptosis in human gingival fibroblasts by activating the Nrf2/HO-1 signaling pathway. Drug Des Dev Ther 14:4901–4913. https://doi.org/10.2147/DDDT.S269223
12. Hu Q, Zhang T, Yi L, Zhou X, Mi M (2018) Dihydromyricetin inhibits NLRP3 inflammasome-dependent pyroptosis by activating the Nrf2 signaling pathway in vascular endothelial cells. BioFactors 44:123–136. https://doi.org/10.1002/biof.1395
13. Gao Z, Sui J, Fan R, Qu W, Dong X, Sun D (2020) Emodin protects against acute pancreatitis-associated lung injury by inhibiting NLPR3 inflammasome activation via Nrf2/HO-1 signaling. Drug Des Dev Ther 14:1971–1982. https://doi.org/10.2147/DDDT.S247103
14. Motterlini R, Foresti R (2014) Heme oxygenase-1 as a target for drug discovery. Antioxid Redox Signal 20:1810–1826. https://doi.org/10.1089/ars.2013.5658
15. Jiang WY, Ren J, Zhang XH, Lu ZL, Feng HJ, Yao XL, Li DH, Xiong R, Fan T, Geng Q (2020) CircC3P1 attenuated pro-inflammatory cytokine production and cell apoptosis in acute lung injury induced by sepsis through modulating miR-21. J Cell Mol Med 24:11221–11229. https://doi.org/10.1111/jcmm.15685
16. Bao X, Zhang Q, Liu N, Zhuang S, Li Z, Meng Q, Sun H, Bai J, Zhou X, Tang L (2019) Characteristics of circular RNA expression of pulmonary macrophages in mice with sepsis-induced acute lung injury. J Cell Mol Med 23:7111–7115. https://doi.org/10.1111/jcmm.14577
17. Matute-Bello G, Downey G, Moore BB, Groshong SD, Matthay MA, Slutsky AS, Kuebler WM, Acute Lung Injury in Animals Study G (2011) An official American Thoracic Society workshop report: features and measurements of experimental acute lung injury in animals. Am J Respir Cell Mol Biol 44:725–738. https://doi.org/10.1165/rcmb.2009-0210ST
18. Yang L, Li D, Zhuo Y, Zhang S, Wang X, Gao H (2016) Protective role of liriodendrin in sepsis-induced acute lung injury. Inflammation 39:1805–1813. https://doi.org/10.1007/s10753-016-0416-1
19. Sadowitz B, Roy S, Gatto LA, Habashi N, Nieman G (2011) Lung injury induced by sepsis: lessons learned from large animal models and future directions for treatment. Expert Rev Anti Infect Ther 9:1169–1178. https://doi.org/10.1586/eri.11.141
20. Potey PM, Rossi AG, Lucas CD, Dorward DA (2019) Neutrophils in the initiation and resolution of acute pulmonary inflammation: understanding biological function and therapeutic potential. J Pathol 247:672–685. https://doi.org/10.1002/path.5221
21. Zeng H, Yang L, Zhang X, Chen Y, Cai J (2018) Dioscin prevents LPSinduced acute lung injury through inhibiting the TLR4/MyD88 signaling pathway via upregulation of HSP70. Mol Med Rep 17:6752–6758. https://doi.org/10.3892/mmr.2018.8667
22. Ye Y, Zhang L, Hu T, Yin J, Xu L, Pang Z, Chen W (2021) CircRNA_103765 acts as a proinflammatory factor via sponging miR-30 family in Crohn's disease. Sci Rep 11:565. https://doi.org/10.1038/s41598-020-80663-w
23. Liu S, Zhang D, Liu Y, Zhou D, Yang H, Zhang K, Zhang D (2020) Circular RNA circ_0001105 protects the intestinal barrier of septic rats by inhibiting inflammation and oxidative damage and YAP1 expression. Gene 755:144897. https://doi.org/10.1016/j.gene.2020.144897
24. Qi D, He J, Wang D, Deng W, Zhao Y, Ye Y, Feng L (2014) 17beta-estradiol suppresses lipopolysaccharide-induced acute lung injury through PI3K/Akt/SGK1 mediated up-regulation of epithelial sodium channel (ENaC) in vivo and in vitro. Respir Res 15:159. https://doi.org/10.1186/s12931-014-0159-1
25. Yang CL, Yang WK, He ZH, Guo JH, Yang XG, Li HB (2021) Quietness of circular RNA circ_0054633 alleviates the inflammation and proliferation in lipopolysaccharides-induced acute lung injury model through NF-kappaB signaling pathway. Gene 766:145153. https://doi.org/10.1016/j.gene.2020.145153
26. Liu Z, He Q, Liu Y, Zhang Y, Cui M, Peng H, Wang Y, Chen S, Li D, Chen L, Xiao Y, Chen W, Wang Q (2021) Hsa_circ_0005915 promotes N, N-dimethylformamide-induced oxidative stress in HL-7702 cells through NRF2/ARE axis. Toxicology 458:152838. https://doi.org/10.1016/j.tox.2021.152838
27. Margueron R, Reinberg D (2011) The Polycomb complex PRC2 and its mark in life. Nature 469:343–349. https://doi.org/10.1038/nature09784
28. Arifuzzaman S, Das A, Kim SH, Yoon T, Lee YS, Jung KH, Chai YG (2017) Selective inhibition of EZH2 by a small molecule inhibitor regulates microglial gene expression essential for inflammation. Biochem Pharmacol 137:61–80. https://doi.org/10.1016/j.bcp.2017.04.016
29. Cai LJ, Tu L, Huang XM, Huang J, Qiu N, Xie GH, Liao JX, Du W, Zhang YY, Tian JY (2020) LncRNA MALAT1 facilitates inflammasome activation via epigenetic suppression of Nrf2 in Parkinson's disease. Mol Brain 13:130. https://doi.org/10.1186/s13041-020-00656-8
30. Ryter SW, Choi AM (2010) Heme oxygenase-1/carbon monoxide: novel therapeutic strategies in critical care medicine. Curr Drug Targets 11:1485–1494. https://doi.org/10.2174/138945011100901485
31. Luo YP, Jiang L, Kang K, Fei DS, Meng XL, Nan CC, Pan SH, Zhao MR, Zhao MY (2014) Hemin inhibits NLRP3 inflammasome activation in sepsis-induced acute lung injury, involving heme oxygenase-1. Int Immunopharmacol 20:24–32. https://doi.org/10.1016/j.intimp.2014.02.017
32. Fei D, Meng X, Kang K, Nan C, Zhao M, Pan S, Gao M, Yang S, Zhao M (2012) Heme oxygenase-1 modulates thrombomodulin

and activated protein C levels to attenuate lung injury in cecal ligation and puncture-induced acute lung injury mice. Exp Lung Res 38:173–182. https://doi.org/10.3109/01902148.2012.660559
33. Gozzelino R, Jeney V, Soares MP (2010) Mechanisms of cell protection by heme oxygenase-1. Annu Rev Pharmacol Toxicol 50:323–354. https://doi.org/10.1146/annurev.pharmtox.010909.105600